Наносистеми, наноматеріали, нанотехнології
Nanosistemi, Nanomateriali, Nanotehnologii
2023, т. 21, № 2, сс. 403–411

© 2023 ІМФ (Інститут металофізики
ім. Г. В. Курдюмова НАН України)
Надруковано в Україні.

PACS numbers: 61.46.Hk, 61.72.Ff, 61.72.Mm, 68.35.Ct, 68.37.Ps, 68.55.J-, 81.15.Cd

Surface Morphology of Thin $ZnGa_2O_4$ Films Obtained by Different Methods

O. M. Bordun[1], V. G. Bihday[1], I. Yo. Kukharskyy[1], I. I. Medvid[1], I. M. Kofliuk[1], I. Yu. Khomyshyn[1], Zh. Ya. Tsapovska[1], and D. S. Leonov[2]

[1]Ivan Franko National University of Lviv,
50, Drahomanov Str.,
UA-79005 Lviv, Ukraine
[2]Technical Centre, N.A.S. of Ukraine,
13, Pokrovska Str.,
UA-04070 Kyiv, Ukraine

Thin films of $ZnGa_2O_4$ are obtained by the method of discrete thermal evaporation and radio-frequency (RF) ion–plasma sputtering. Studies of the surface morphology of the obtained films by atomic force microscopy (AFM) show that the transition from discrete thermal evaporation to RF sputtering leads to increases in the average grain diameters by a factor of two and in grain heights by more than a factor of three. As established, the distribution of grains in terms of their diameters is multimodal and has several centres, which in both methods of preparation correlate as small integers. This indicates the growth of small grains among themselves with the formation of large grains.

Методом дискретного термічного випаровування та високочастотного (ВЧ) йонно-плазмового розпорошення одержано тонкі плівки $ZnGa_2O_4$. Дослідження морфології поверхні одержаних плівок методом атомно-силової мікроскопії (АСМ) показали, що з переходом від дискретного термічного випаровування до ВЧ-розпорошення відбувається зростання розмірів середніх діяметрів зерен у два рази та висот зерен у понад три рази. Встановлено, що розподіл зерен за величиною їхніх діяметрів є багатомодальним і має декілька центрів, які в обох методах одержання співвідносяться як малі цілі числа. Це свідчить про зростання малих зерен між собою з утворенням великих зерен.

Key words: zinc gallate, thin films, nanocrystallites.

Ключові слова: ґалат Цинку, тонкі плівки, нанокристаліти.

(Received 28 March, 2023)

1. INTRODUCTION

Due to the wide range of applications in optoelectronics and device engineering, researchers in recent years have shown interest in thin films of metal-oxide materials. Among them, thin films based on zinc gallate $ZnGa_2O_4$ have a significant place due to their good optical, dielectric, and operational properties [1–4]. In addition, both pure and activated $ZnGa_2O_4$ films exhibit good luminescent properties and are widely investigated for practical use in electronic–optical devices [5–7]. The presence of nanocrystalline components that form such films ensures high efficiency and stability of the luminescence of these materials and expands the potential areas of their use. Analysis of the dimensional, morphological, and structural characteristics of nanoparticles indicates that they depend significantly on the method and conditions of obtaining nanostructures [8–10]. This has led to the study of the surface morphology of thin films of $ZnGa_2O_4$ obtained by the method of thermal discrete evaporation in vacuum and radio-frequency (RF) ion–plasma sputtering. Atomic force microscopy (AFM), which was used in this study, belongs to the methods of high-resolution capability to determine the size and morphology of nanoparticles.

2. EXPERIMENTAL TECHNIQUE

Thin films of $ZnGa_2O_4$ with a thickness of 0.3–1.0 μm were obtained by discrete evaporation in vacuum and RF ion–plasma sputtering on substrates of fused quartz ν-SiO_2. The RF sputtering was carried out in an argon atmosphere in a system using the magnetic field of external solenoids for compression and additional ionization of the plasma column. The initial raw material was a mixture of ZnO and Ga_2O_3 oxides with a stoichiometric composition of the OSCh brand (especially pure). The deposition of films on substrates was carried out at room temperature. After the films were deposited, they were heat treated in air at a temperature of 1000–1100°C for 2–2.5 hours.

X-ray diffraction studies showed the presence of a polycrystalline structure with a predominant orientation in the planes (022), (113), (004), and (333). The characteristic diffraction patterns of thin films of $ZnGa_2O_4$ were previously presented in our work [11], and typical electron diffraction patterns are presented in the work [12]. The obtained diffraction patterns did not reveal reflections that did

not correspond to $ZnGa_2O_4$, indicating the absence of other phases. All diffraction maxima are identified according to the selection rules and belong to the space group $Fd3m$, which indicates the cubic structure of the obtained films.

Elemental analysis of samples at various points on the surface of films was carried out using the OXFORD INCA Energy 350 energy-dispersive spectrometer. The calculations confirmed that the percentage composition of the components in the obtained films corresponded to their percentage composition in the $ZnGa_2O_4$ compound.

The morphology of the film surfaces was investigated using the Solver P47 PRO atomic force microscope. The processing of experimental data and the calculation of surface morphology parameters were carried out using the Image Analysis 2 software package.

3. RESULTS AND DISCUSSION

Microphotographs of the surface of thin $ZnGa_2O_4$ films obtained by the method of discrete evaporation and RF magnetron sputtering are presented in Fig. 1 using AFM. The topography of the samples was quantitatively characterized by standard parameters such as the average grain diameter and height, root-mean-square roughness,

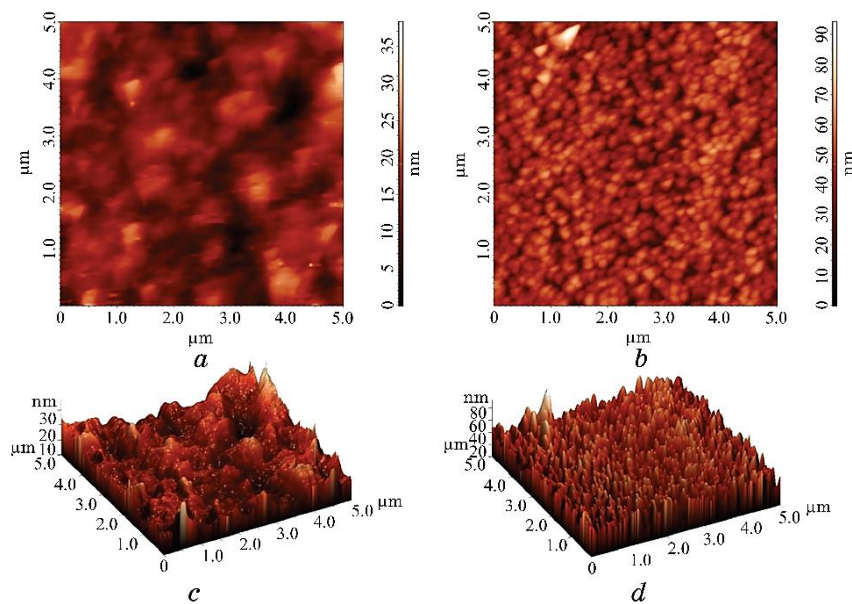

Fig. 1. Image of the surface morphology of a thin $ZnGa_2O_4$ film obtained by discrete evaporation (*a*, *c*) and RF ion–plasma sputtering (*b*, *d*). Images *a* and *b* are two-dimensional, *c* and *d* are three-dimensional.

which were calculated from AFM data for regions of the same size (5000×5000 nm). The characteristic parameters of the thin $ZnGa_2O_4$ films obtained by different methods are given in Table.

As can be seen from Fig. 1, *c*, *d*, the $ZnGa_2O_4$ films obtained by the method of discrete thermal evaporation method have a more uneven surface with smaller nanocrystalline formations observed. Specifically, our results show that, with transition from discrete thermal evaporation to RF sputtering, the sizes of nanocrystals forming the structure of thin $ZnGa_2O_4$ films increase. Interestingly, this reveals a pattern in the morphology of the surface of the obtained films. As shown in Table, the average grain diameter on the surface of the films obtained by RF sputtering is twice as large as the average grain diameter on the surface of the films obtained by discrete thermal evaporation. Additionally, the root-mean-square roughness, average height, and maximum height of the grains on the surface of the thin $ZnGa_2O_4$ films obtained by RF sputtering are more than three times greater than those obtained by discrete thermal evaporation are.

To analyse the obtained results, we use the results of the classical work by B. A. Movchan and A. V. Demchishin [13], according to the classification of the microstructure state of thin films. A whole series of subsequent works, including those using computer modelling methods, took this work as a basis and confirmed its positions [14–18]. According to [13], for deposited metal and oxide films, including $ZnGa_2O_4$, there are three different temperature intervals. These intervals are separated by temperatures $T_1 \approx 0.3T_{mt}$ and $T_2 \approx 0.5T_{mt}$, where T_{mt} is the melting temperature of the deposited material. In the highest temperature zone III ($T > T_2$), large crystallites are formed, and their formation is associated with volume diffusion processes. A columnar structure is formed in temperature zone II, which is associated with surface self-diffusion. Low-temperature precipitation occurs in the low-temperature zone I ($T < T_1$). In this region, the film surface is formed from dome-shaped microcrystallites that have a block structure and pores along the boundaries. As the temperature decreases, the sizes of the crystallites and block structure decrease [13]. It should be noted that

TABLE. Parameters of crystalline grains of thin $ZnGa_2O_4$ films.

Parameter	Discrete evaporation	RF sputtering
Average grain diameter, nm	78.0	157.0
Average grain height, nm	9.0	42.4
Root-mean-square roughness, nm	3.3	10.2
Maximum grain height, nm	30.1	94.0

the physical mechanisms by which the microstructure of thin films is formed in the low-temperature zone I have not yet been established.

Differences in the structure of the obtained thin $ZnGa_2O_4$ films are due to differences in the process of condensation of materials during RF ion–plasma sputtering and thermal vacuum discrete evaporation. During ion sputtering, there is no critical temperature or critical density of the particle beam, so film condensation occurs at any practically possible beam densities and substrate temperatures [19], which is due to the high energy of the sputtered particles. The average energy of sputtered particles obtained by ion sputtering methods is one to two orders of magnitude higher than that of particles evaporated at ≈ 2000 K. Specifically, according to [20], these values are of 3–5 eV and 0.15 eV, respectively. Such differences lead to differences in the formation of the structure of deposited films. In addition, significant influence on the formation of the film structure is the bombardment of the substrate with secondary electrons, negative ions, and atoms of the sprayed material, which leads to an increase in the temperature of the film. Based on our results of the investigation of the morphology of the surface of thin films of $ZnGa_2O_4$, we can suggest that, as a result of radio-frequency ion–plasma sputtering, the temperature of film formation begins to exceed $0.3T_{mt}$, and as a result, a columnar structure begins to form. This can be seen from the fact that when transitioning from discrete evaporation to radio-frequency ion–plasma sputtering, the average grain size doubles, and the height of the grain increases by more than three times. The typical height distribution of grains on the AFM images of thin $ZnGa_2O_4$ films obtained by various methods is shown in Fig. 2.

The observed increase in grain size in thin films of $ZnGa_2O_4$ upon

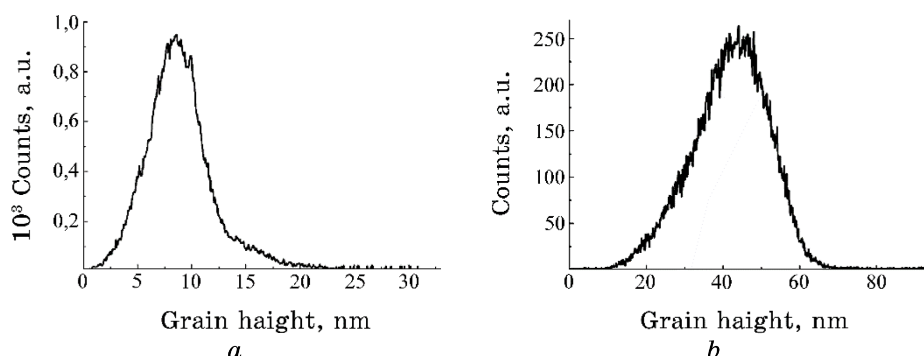

Fig. 2. Grain height distribution in AFM images of thin $ZnGa_2O_4$ films obtained by (*a*) discrete evaporation and (*b*) RF sputtering.

transition from discrete evaporation to RF sputtering (Table) indicates the possibility of surface transformation of $ZnGa_2O_4$ film into a more nanostructured state through the crystallization of the surface layer during RF ion–plasma deposition.

The characteristic distributions of grain diameter sizes in thin films of $ZnGa_2O_4$ obtained by different methods are presented in Fig. 3.

The results show that for the surface of $ZnGa_2O_4$ films obtained by different methods, a complex multimodal distribution is observed. This distribution is characterized by a set of maxima, the position of which is determined by the film preparation method. In particular, during discrete evaporation, the most intense maximum appears at 37 nm and then several weaker maxima are recorded at 110, 190, 265, and 370 nm. During RF ion–plasma sputtering, the main maximum appears at 120 nm, and then, a set of maxima is observed at 233, 354, and 480 nm.

The growth of crystalline grains and the evolution of crystal structures were analysed in detail [21]. This work demonstrates that polycrystalline thin films with thicknesses not exceeding 1 μm often have 2*D*-like structures, for which most grain boundaries are perpendicular to the film surface. Most of the materials analysed in [21] have nonequilibrium grains with sizes smaller than the film thickness, which form two-dimensional structures only after annealing. However, the formation of grains in thin films is difficult to describe accurately based on model assumptions or analyses of experiments on other structures.

In some cases, further grain growth is observed due to ‘abnormal’ or predominant growth of several grains, which usually have specific crystallographic orientation relationships with respect to the plane of the substrate surface. When the number of growing grains leads to a ‘matrix’ of grains with static boundaries, a bimodal distribution of grain sizes develops, which is called secondary grain growth [22]. This situation, for example, is manifested in thin Y_2O_3:Eu films obtained by RF ion–plasma sputtering, depending on the concentration of the Eu^{3+} activator [23]. Abnormally growing grains often have limited or homogeneous texture. Secondary grain growth in thin films usually involves the evolution of texture distribution as well as the evolution of grain size distribution.

The situation with the growth of grains that form thin $ZnGa_2O_4$ films looks somewhat more complicated than the examples given above.

As can be seen from Fig. 3, grain growth during the growth of the $ZnGa_2O_4$ film leads to the existence of several peaks and, accordingly, distributions. The analysis shows that for the cross section near the surface in films obtained by discrete evaporation, five dis-

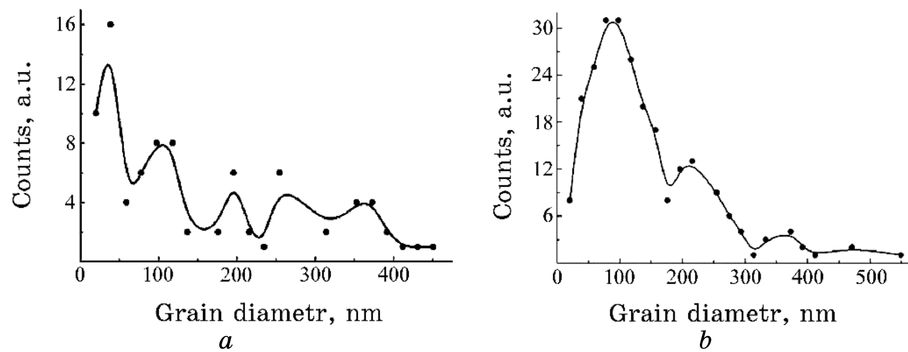

Fig. 3. The distribution of grain diameters and the approximated diameter distribution in AFM images of thin $ZnGa_2O_4$ films obtained by discrete evaporation (*a*) and RF sputtering (*b*) were calculated.

tributions are observed with centres at 37, 110, 190, 265, and 370 nm. For $ZnGa_2O_4$ films obtained by RF sputtering, four distributions are observed with centres at 120, 233, 364, and 480 nm. Interestingly, the centres of the distributions in both types of films are related as small integers. For $ZnGa_2O_4$ films obtained by discrete evaporation, this ratio can be expressed as 1:3:5:7:10, and for films obtained by RF sputtering, it is expressed as 1:2:3:4. Such a ratio between the centres of the distributions indicates that the growth of grain diameters near the surface of $ZnGa_2O_4$ films occurs by the growth of small grains to form larger ones.

4. CONCLUSIONS

It has been found that polycrystalline $ZnGa_2O_4$ films are formed from nanosize grains during radio-frequency ion–plasma sputtering and discrete thermal evaporation.

According to the AFM data, a transition from discrete thermal evaporation to radio-frequency sputtering leads to an increase in the average grain size diameter by a factor of two and a more than threefold increase in grain height. This is attributed to an increase in substrate temperature during radio-frequency sputtering and an increased influence of surface self-diffusion, resulting in a columnar structure of the thin $ZnGa_2O_4$ films obtained by this method.

Based on the analysis of the grain-size distribution results, it has been established that in the thin $ZnGa_2O_4$ films formed by both discrete evaporation and radio-frequency sputtering, multimodal distributions are observed, with the distribution centres corresponding to small integers. This indicates the growth of small grains into large ones.

REFERENCES

1. L. Zou, X. Xiang, M. Wei, F. Li, and D. G. Evans, *Inorg. Chem.*, **47**, No. 4: 1361 (2008); https://doi.org/10.1021/ic7012528
2. W. Zhang, J. Zhang, Yu. Li, Z. Chen, and T. Wang, *Appl. Surf. Sci.*, **256**, No. 14: 4702 (2010); https://doi.org/10.1016/j.apsusc.2010.02.077
3. J. S. Kim, J. S. Kim, T. W. Kim, H. L. Park, Yo. G. Kim, S. K. Chang, and S. D. Han, *Solid State Commun.*, **131**, No. 8: 493 (2004); https://doi.org/10.1016/j.ssc.2004.06.023
4. O. M. Bordun, V. G. Bihday, and I. Yo. Kukharskyy, *J. Appl. Spectrosc.*, **80**, No. 5: 721 (2013); https://doi.org/10.1007/s10812-013-9832-2
5. M. Orita, M. Takeuchi, H. Sakai, and H. Tanji, *Jpn. J. Appl. Phys.*, **34**, No. 11B: L1550 (1995); https://doi.org/10.7567/JJAP.34.L1550
6. Ph. D. Rack, J. J. Peterson, M. D. Potter, and W. Park, *J. Mater. Res.*, **16**, No. 5: 1429 (2001); https://doi.org/10.1557/JMR.2001.0199
7. P. Dhak, U. K. Gayen, S. Mishra, P. Pramanik, and A. Roy, *J. Appl. Phys.*, **106**, No. 6: 063721 (2009); https://doi.org/10.1063/1.3224866
8. O. M. Bordun, I. I. Kukharskii, T. M. Yaremchuk, and S. I. Gaidai, *J. Appl. Spectosc.*, **71**, No. 3: 382 (2004); https://doi.org/10.1023/B:JAPS.0000039965.10766.c8
9. Z. Chi, T. Tchelidze, C. Sartel, T. Gamsakhurdashvili, I. Madaci, H. Yamano, V. Sallet, Y. Dumont, A. Pérez-Tomás, F. Medjdoub, and E. Chikoidze, *J. Phys. D: Appl. Phys.*, **56**: 105102 (2023); https://doi.org/10.1088/1361-6463/acbb14
10. A. K. Singh, Ch.-Ch. Yen, and D.-S. Wuu, *Results in Physics*, **33**: 105206 (2022); https://doi.org/10.1016/j.rinp.2022.105206
11. O. M. Bordun, I. Yo. Kukharskyy, and V. G. Bihday, *J. Appl. Spectrosc.*, **78**, No. 6: 922 (2012); https://doi.org/10.1007/s10812-012-9555-9
12. V. Bondar, L. Akselrud, M. Vasyliv, M. Grytsiv, Yu. Dubov, S. Popovich, V. Davydov, I. Kucharsky, and N. Lutsyk, *Functional Materials*, **6**, No. 3: 510 (1999).
13. B. A. Movchan and A. V. Demchychyn, *Fiz. Met. Metalloved.*, **28**, No. 4: 654 (1969) (in Russian).
14. I. Heyvaert, J. Krim, C. Van Haesendonck, and Y. Bruynseraede, *Phys. Rev. E*, **54**, No. 1: 349 (1996); https://doi.org/10.1103/PhysRevE.54.349
15. K. L. Ekinci and J. M. Valles, *Acta Mater.*, **46**, No. 13: 4549 (1998); https://doi.org/10.1016/S1359-6454(98)00145-1
16. J. G. Amar, *Phys. Rev. B*, **54**, No. 20: 14742 (1996); https://doi.org/10.1103/PhysRevB.54.14742
17. R. W. Smith and D. J. Srolovitz, *J. Appl. Phys.*, **79**, No. 3: 1448 (1996); https://doi.org/10.1063/1.360983
18. B. S. Bunnik, C. de Hoog, E. F. C. Haddeman, and B. J. Thijsse, *Nucl. Instrum. and Meth. Phys. Res. B*, **187**, No. 1: 57 (2002); https://doi.org/10.1016/S0168-583X(01)00849-7
19. V. E. Yurasova and V. A. Eltekov, *Vacuum*, **32**, No. 7: 399 (1982); https://doi.org/10.1016/0042-207X(82)94064-7
20. B. S. Danilin, *Primenenie Nizkotemperaturnoy Plazmy Dlya Naneseniya Tonkikh Plyonok* [The Use of Low-Temperature Plasma for the Deposition of Thin Films] (Moskva: Ehnergoatomizdat: 1989) (in Russian).

21. C. V. Thompson, *Solid State Physics* (Eds. H. Ehrenreich and F. Spaepen) (Academic Press: 2001).
22. C. V. Thompson, *J. Appl. Phys.*, **58**, No. 2: 763 (1985); https://doi.org/10.1063/1.336194
23. O. M. Bordun, I. O. Bordun, I. M. Kofliuk, I. Yo. Kukharskyy, I. I. Medvid, Zh. Ya. Tsapovska, and D. S. Leonov, *Nanosistemi, Nanomateriali, Nanotehnologii*, **20**, Iss. 1: 91 (2022); https://doi.org/10.15407/nnn.20.01.091